BJR

https://doi.org/10.1259/bjr.20210539

Received: 29 April 2021 | Revised: 13 October 2021 | Accepted: 17 November 2021

Cite this article as:
Cho H, Kim CK, Park H. Overview of radiomics in prostate imaging and future directions. *Br J Radiol* 2022; **95**: 20210539.

INNOVATIONS IN PROSTATE CANCER SPECIAL FEATURE: REVIEW ARTICLE

Overview of radiomics in prostate imaging and future directions

[1,2]HWAN-HO CHO, [3]CHAN KYO KIM and [2,4]HYUNJIN PARK

[1]Department of Electrical and Computer Engineering, Sungkyunkwan University, Suwon, Korea
[2]Center for Neuroscience Imaging Research, Institute for Basic Science, Suwon, Korea
[3]Department of Radiology and Center for Imaging Science, Samsung Medical Center, Sungkyunkwan University School of Medicine, Seoul, Korea
[4]School of Electronic and Electrical Engineering, Sungkyunkwan University, Suwon, Korea

Address correspondence to: Prof Hyunjin Park
E-mail: *hyunjinp@skku.edu*

ABSTRACT

Recent advancements in imaging technology and analysis methods have led to an analytic framework known as radiomics. This framework extracts comprehensive high-dimensional features from imaging data and performs data mining to build analytical models for improved decision-support. Its features include many categories spanning texture and shape; thus, it can provide abundant information for precision medicine. Many studies of prostate radiomics have shown promising results in the assessment of pathological features, prediction of treatment response, and stratification of risk groups. Herein, we aimed to provide a general overview of radiomics procedures, discuss technical issues, explain various clinical applications, and suggest future research directions, especially for prostate imaging.

INTRODUCTION

Over the past decade, the assessment of tumor characteristics through medical imaging and advanced analysis techniques has undergone transformative changes towards personalized medicine. In particular, radiomics extracts high-dimensional features from raw imaging data and builds an analytical model based on data mining to improve clinical decision-making.[1,2] Initial efforts focused on quantifying intratumoral heterogeneity using various texture features from imaging modalities such as X-ray, ultrasound, CT, and MRI, which span the lung, breast, and prostate.[3–7] The current set of radiomics features goes beyond texture and includes 2D/3D shape features, signal intensity features from the histogram, and deep learning (DL) inspired features.[1] Some studies have added new features that reflect prior knowledge to enhance the feature set. For example, features specific to the tumor margins have been proposed for lung cancer.[8] After appropriate data mining and model building procedures, radiomics offers improvements in the assessment of pathological features, prediction of treatment response, stratification of risk groups, etc.

Radiomics and radiogenomics have made significant contributions to all subdisciplines in radiology; urologic radiology is no exception. In this study, we aimed to provide a general overview of radiomics procedures, discuss technical issues, explain various clinical applications, and suggest future research directions, especially for prostate imaging. We mainly focused on radiomics.

General overview of radiomics procedures

This section outlines the standard steps involved in radiomics studies, as shown in Figure 1. We first start with procedures common to all subdisciplines in radiology and then describe prostate-specific issues.

Image acquisition and preprocessing

As with any study, the first step is to acquire the appropriate imaging data. Sufficient samples should be collected to obtain statistically valid results.[9] This is important because we deal with hundreds to thousands of features in radiomics, which makes it especially vulnerable to small n, large p issues. Different imaging parameters and scanner types affect the raw data and thus lead to increased feature variability. The best practice is to adhere to a strict imaging protocol to reduce variability in imaging parameters. However, this could be unrealistic in multicenter studies, where differences in imaging parameters are expected. One can use a similar data setting between multicenter cohorts or apply a retrospective harmonization method to reduce

Figure 1. The overall workflow of radiomics.

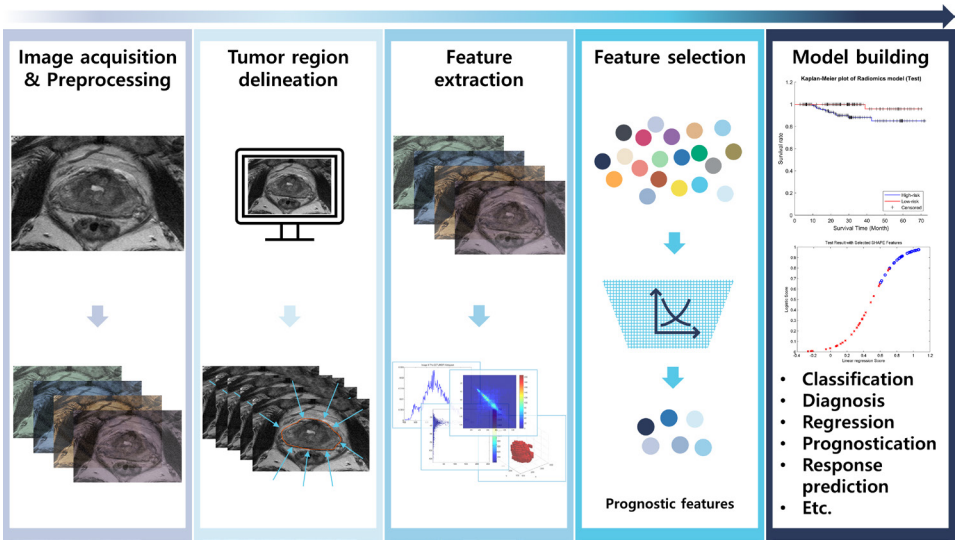

intercenter variability.[10–13] To handle differences in image resolution, the data can be resampled to a common isotropic resolution (*e.g.* $1 \times 1 \times 1\,mm^3$). If different imaging protocols were used in one study, it should be noted to improve the reproducibility of future studies.

In the preprocessing step, registration, filtering, and intensity normalization are commonly performed.[14,15] Image registration is typically performed to align multimodal images. Filtering, in the form of smoothing, can be performed to reduce noise. Intensity normalization can be used for stable feature extraction.[16–18] It is important to ensure that the inherent property of the imaging modality is retained after preprocessing. Dynamic contrast-enhanced MRI should be normalized considering all phases because normalizing individual phases might remove the time-varying enhancing pattern. The application of inhomogeneity correction for MRI is controversial because it may change the intensity profile.[19,20] However, it might increase the feature stability across patients; thus, some studies still adopt it.[21,22]

Delineation of the region of interest

Radiomics is a focal analysis method in which regions of interest (ROIs) should be specified. Typically, the tumor region is specified by manual, automatic, or semi-automatic methods. However, normal regions could be analyzed based on the study goals. Manual specification fully reflects expert knowledge but may suffer from inter- and intraobserver variability. The automatic method applies a computer-based segmentation algorithm; thus, it is fast and leads to no or reduced variability. From classical computer vision, region-growing, watershed, active contour algorithms have been widely used for segmentation.[23–25] Recently, U-net-based deep learning has been adopted for prostate segmentation.[26] The semi-automatic method allows users to interactively modify the algorithm-generated ROI, and thus, is the middle ground between the manual and automatic methods. Additionally, this is the preferred method because it is faster than the manual method and allows modification of the results by experts.

Recent radiomics studies went beyond the tumor region and attempted to quantify the peritumor region so that the surrounding microenvironment could be modeled.[3,27–32] This was performed by expanding the tumor ROI. Prostate radiomics can certainly benefit from this; a recent study reported that peritumoral radiomics can yield results that are independent predictors for risk stratification in prostate cancer.[33] Active research is ongoing regarding the extent to which we probe (*i.e.* 1 to 5 mm) beyond the tumor boundary.

Feature extraction

In the feature extraction step, researchers extracted hundreds to thousands of features belonging to different categories from the prespecified ROIs. Most studies have the following three categories, as shown in Table 1[34,35]: histogram-based features, texture features, and morphological features. In addition to the standard set of features, each study might consider additional options, such as margin features. The features are defined mathematically; this lends the possibility of interpreting features physically and biologically.

The histogram-based features are computed from the intensity histogram of the ROI and include the mean, variance, kurtosis, etc. Texture features are the main focus of radiomics studies since they quantify intratumoral heterogeneity. Typically, they are computed from the gray-level co-occurrence matrix (GLCM) and gray-level size zone matrix, which model intervoxel heterogeneity.[36] The morphological features (*e.g.* roundness) quantify the tumor shape in 2D or 3D. They are direct extensions of semantic features measured by experts, except that they are mathematically defined and continuous-valued. For example, roundness is measured in a binary fashion (round *vs* non-round) in semantic features, while roundness in radiomics is a continuous value between 0 and 1 defined mathematically.

New radiomics features have been actively developed. Features tailored to tumor margins have shown promising results.[8] Texture based on the orientation of the intensity gradient

Table 1. Radiomics features based on pyradiomics[34] documentation

Category	Measure	Features
Histogram	Histogram	10Percentile, 90Percentile, Energy, Entropy, Interquartile Range, Kurtosis, Maximum, Mean Absolute Deviation, Mean, Median, Minimum, Range, Robust Mean Absolute Deviation, Root Mean Squared, Skewness, Total Energy, Uniformity, Variance
Texture	GLCM	Autocorrelation, Cluster Prominence, Cluster Shade, Cluster Tendency, Contrast, Correlation, Difference Average, Difference Entropy, Difference Variance, Inverse Difference, Inverse Difference Moment, Inverse Difference Moment Normalized, Inverse Difference Normalized, Informational Measure Of Correlation1, Informational Measure Of Correlation2, Inverse Variance, Joint Average, Joint Energy, Joint Entropy, Maximal Correlation Coefficient, Maximum Probability, Sum Average, Sum Entropy, Sum Squares
Texture	GLSZM	Gray Level Non-Uniformity, Gray Level Non-Uniformity Normalized, Gray Level Variance, High Gray Level Zone Emphasis, Large Area Emphasis, Large Area High Gray Level Emphasis, Large Area Low Gray Level Emphasis, Low Gray Level Zone Emphasis, Size Zone Non-Uniformity, Size Zone Non-Uniformity Normalized, Small Area Emphasis, Small Area High Gray Level Emphasis, Small Area Low Gray Level Emphasis, Zone Entropy, Zone Percentage, Zone Variance
Morphological	-	Elongation, Flatness, Least Axis Length, Least Axis Length, Maximum 2D Diameter Column, Maximum 2D Diameter Row, Maximum 2D Diameter Slice, Maximum 2D Diameter, Mesh Volume, Sphericity, Surface Area, Surface Volume Ratio, Voxel Volume

GLCM, gray-level co-occurrence matrix; GLSZM, gray-level size zone matrix.

might add complementary information in addition to the conventional GLCM.[37] One study quantified the structural deformation of tumors according to tumor progression.[38] Some studies have extracted vessel features based on tubular structure analysis.[39,40] These new features are relatively under-explored for prostate imaging and are promising avenues for future research.

Feature selection

The feature selection step involves selecting important features from a pool of hundreds to thousands of features. This is because it is infeasible to use many potentially correlated features from the extraction step. The goal is to obtain a compact set of features with low redundancy. The selected features are sometimes referred to as radiomics signatures. Borrowing from machine learning, there are four feature selection methods: filter, wrapper, embedded, and dimension reduction methods.[41] The filter method selects the most meaningful features by measuring the direct associations between the features and outcomes. This does not consider collinearity among the selected features and could be undesirable. The wrapper method seeks optimal features by evaluating possible feature sets using machine learning models. It has high computational costs and tends to overfit the training data. Support vector machine-based recursive feature elimination[42] and stepwise regression[43] are widely used. The embedded method has explicit feature selection during the model-building procedure. Typically, regularized regressions in the form of the least absolute shrinkage and selection operator (LASSO)[44] and ridge regression belong to this category. LASSO theoretically guarantees the maximum orthogonality between features and derives sparse results. Therefore, it is widely used in radiomics. Dimension reduction projects high-dimensional features onto a different computational space where a compact representation is possible. Methods such as principal component analysis[45] are widely used. However, once the radiomics features are mapped onto a different space, it is difficult to interpret them.

Model building

Important features were identified and are used to build various machine-learning models suitable for each study. They can be broadly grouped into classification, regression, and survival models.[1] The classification assigns category labels (*e.g.* non-responding *vs* responding) to patients, and thus could be used for many purposes, including treatment response, tumor staging, and subtyping. Common models include the support vector machine,[46] random forest,[47] linear discriminant analysis,[48] and logistic regression.[49] Regression is used when the target is continuously valued (*i.e.* prostate antigen levels). Depending on the characteristics of the target, nonlinear regression can be applied. Survival analysis is mostly performed using Cox's proportional hazard model with the selected features.[50]

Integrating genomics information with radiomics

Radiogenomics itself is a distinct research topic; thus, a comprehensive review is beyond the scope of this study.[51,52] Still, we explain a few methods for integrating genomic features during the various steps of radiomics. First, radiogenomics is widely used to obtain an in-depth understanding of tumors by exploring the association between radiomics and genomics. It is possible to explore genomic characteristics based on the radiomics signature.[53–55] Similarly, it is also possible to conduct radiomics modeling based on genomics signature.[56–58] Both approaches fix one set of information and use it to explore another set of information. Second, after separately performing radiomics and genomics modeling, the final modeling can be performed by combining the results of the two models.[59] In addition, enrichment scores may be added as an additional feature in classification or regression models.

TECHNICAL ISSUES

In this section, we discuss some technical issues and limitations of radiomics. First, the most well-known issue is feature reproducibility stemming from variability in the imaging protocol.[9–12,17,60] Unstandardized imaging parameters, scanner-dependent

characteristics, and variability in contrast agents lead to changes in the raw data, resulting in decreased feature reproducibility. This problem is particularly serious in MRI because CT can guarantee a basic level of stability due to the physical unit of Hounsfield.[61] General structural MRI has no standardized units that can be shared by different sites. Even MRI images with the same sequence may have differences in the raw imaging data.[62] These limitations can be partially overcome by quantitative MRI such as apparent diffusion coefficient imaging.[63] Still, we should strive towards a standardized imaging protocol so that radiomics built from one setting can be generalized to other scenarios. There are methods to improve the reproducibility of the features. Retrospective harmonization to regress out imaging protocol-related covariates is widely used.[13] Normalizing the intensities using histogram equalization is another common approach. In addition, dynamic MRI should be performed to ensure accurate timing of the various phases. In a real clinical setting, it is difficult to avoid feature reproducibility problems; however, we should strive to reduce it as much as possible towards a reproducible and generalizable radiomics model.

The second issue is commonly referred to as the curse of dimensionality.[64–66] Radiomics features can be hundreds to thousands or more, depending on the goal of the study. The feature dimension grows quickly if genomics is involved, resulting in millions of features. The incredibly high dimensionality of the feature space requires large data samples for proper modeling. However, owing to practical clinical limitations, we rarely have sufficient samples. There are a few radiomics studies in which the sample size exceeded 500.[67] One way to tackle this problem is to limit the number of features. Many researchers believe that more features are always better. However, this is only valid if sufficient samples are available. With limited samples, researchers can choose important categories of features that worked well in previous studies instead of using the full suite of features. Another side-effect of insufficient samples is overfitting. Using limited samples might lead to modeling results that overfit the given training data. This can be partly mitigated by cross-validation, but the better option is to use independent external validation data.[68] Overfitting is a major issue that is beyond the scope of this study, and readers can study other excellent literature.[1,67]

APPLICATION OF RADIOMICS IN PROSTATE CANCER

Classification of pathological features

In this section, we survey recent studies of radiomics in prostate imaging (Table 2). Many studies have applied radiomics to prostate-related classification tasks. Bernatz et al[69] adopted radiomics features and principal component analysis to discriminate groups stratified by Gleason scores using multiparametric MRI. Chaddad et al[70] conducted a similar study using intermodality

Table 2. Recent studies of radiomics/radiogenomics on prostate cancer

Application	Reference	Imaging modality	Study target	RQS
Classification				
	Bernatz et al.[69]	T2, ADC, DCE-T1, T1	Gleason Grade Group (1,2 *vs* 3,4,5)	12
	Chaddad et al.[70]	T2, ADC	Gleason Grade Group (1 *vs* 2 *vs* 3,4,5)	13
	Chen et al.[71]	T2, ADC	Gleason Score Group (>6 or not)	14
	Gong et al.[72]	T2, ADC	Gleason Score Group (>7 or not)	15
	Shiradkar et al.[21]	T2, ADC	Biochemical recurrence	17
	Zamboglou et al.[73]	PET	Cancer or not, Gleason Score Group (>7 or not), Stage (pN1 *vs* pN0)	16
Regression				
	Hectors et al.[74]	T2, ADC	Gleason Score, Gene signature association	16
	Krauss et al.[22]	T2	Prostate-specific antigen serum level	14
Survival analysis				
	Bourbonne et al.[75]	DCE-T1, T2, ADC	Biochemical relapse-free survival	15
	Mo et al.[76]	CT (Con/non-Con)	Progression-free survival after chemotherapy	18
Radiogenomics				
	McCann et al.[77]	DCE-T1, T2, ADC	Radiomics-Gene expression association	-
	Stoyanova et al.[78]	DCE-T1, T2, ADC	Radiomics-Gene expression association	-
	Kesch et al.[79]	Ga-PSMA-PET/CT	Radiomics-Genomic index association	-
	Fischer et al.[80]	T2	Combining pretreatment, clinical, genomics pathway, and radiomics feature to predict pathological stage	-

ADC, apparent diffusion coefficient; DCE, dynamic contrast-enhanced; PET, positron emission tomography; PSMA, prostate-specific membrane antigen.
RQS, radiomics quality score

texture features in addition to conventional GLCM texture features to classify groups stratified by Gleason scores using T_2 weighted MRI images and apparent diffusion coefficient (ADC) maps. Chen et al[71] compared prostate imaging reporting and data system (PI-RADS) with radiomics in differentiating high-grade and low-grade Gleason score groups using T2 images and ADC maps. In this study, the authors adopted an augmentation technique, called the synthetic minority oversampling technique, to boost samples in the minority class. Results have shown that the radiomics model was better than the conventional PI-RADS. Additionally, Gong et al[72] also performed the same classification task using additional clinical information and showed that both radiomics and clinical information lead to better classification. This study also used T2 and ADC maps. Shiradkar et al[21] showed that it is feasible to predict biochemical recurrence using recently proposed texture features based on the orientation of the intensity gradient in T2 images and ADC maps. Many studies have used MRI, but some have used position emission tomography (PET). Zamboglou et al[73] demonstrated the effectiveness of radiomics modeling obtained from the gross tumor volume of PET images. In this study, the authors showed that PET radiomics can be used to distinguish between cancer and non-cancer groups, groups stratified by Gleason scores, and different stages.

Regression and survival models

Some studies performed regression tasks using radiomics for prostate imaging (Table 2). Hectors et al[74] confirmed a linear association between radiomics features from T2 and ADC maps, and as well as clinical outcomes such as Gleason scores. Krauss et al[22] built a radiomics model to predict antigen serum levels and compared it with conventional volume measurements in the transition zone using T2 MRI. Some studies have shown that survival analysis using a radiomics approach is feasible. Bourbonne et al[75] built a multivariate Cox model using radiomics features to evaluate recurrence risks from MRI. It was shown that prediction of biochemical recurrence was possible; stratification of risk groups for biochemical relapse-free survival was also possible. Similarly, Mo et al[76] showed that radiomics using both contrast-enhanced and regular CT images can be used to create a progression-free survival model after chemotherapy for stratifying risk groups.

Radiogenomics

Radiogenomics combines high-dimensional radiomics features with genomic features, another high-dimensional feature, to better probe tumor characteristics.[51,52] This approach allows us to establish links between macroscale imaging and microscale genetic information, which might lead to a better understanding of the underlying tumor biology.

Some studies have applied radiogenomics to prostate imaging. McCann et al[77] and Stoyanova et al[78] explored the relationships between radiomics features and prognostic gene expression in the form of gene-associated radiomics signatures. Using a more advanced technique, Kesch et al[79] found that a cluster formed by grouping similar radiomics features was related to a well-known genomics index. Fischer et al[80] integrated three types of pretreatment information, clinical information, genomics pathway, and radiomics features to predict the pathological stage. The molecular characteristics of each stage were evaluated through the analysis of genes and miRNAs; the association between biomarkers and imaging features was also analyzed. Radiogenomics studies in prostate imaging are relatively scarce compared to other organs and thus, are a rich avenue for future research exploring radiomics-genomics associations.

Table 3. Adherence rate according to the 6 key categories and 16 items of RQS

Category/Item	Adherence rate
Average of 16 items	41.9%
Category 1: Protocol quality and stability in image and segmentation	34.0%
Protocol quality	50.0%
Test–retest	0.0%
Phantom study	0.0%
Multiple segmentation	70.0%
Category 2: Feature selection and validation	66.3%
Feature reduction or adjustment of multiple testing	100.0%
Validation	46.0%
Category 3: Biologic/clinical validation and utility	86.7%
Multivariate analysis with non-radiomics features	90.0%
Biologic correlates	50.0%
Comparison to 'gold-standard'	90.0%
Potential clinical utility	100.0%
Category 4: Model performance index	54.0%
Discrimination statistics	90.0%
Calibration statistics	10.0%
Cut-off analysis	70.0%
Category 5: High level of evidence	0.0%
Prospective study	0.0%
Cost-effective analysis	0.0%
Category 6: Open science and data	5.0%

RQS, radiomics quality score.

FUTURE DIRECTIONS

Evaluation of existing literature

To provide objective interpretations, we evaluated the studies in Table 2 with radiomics quality score (RQS).[81] We evaluated RQS for pure-radiomics studies because it may be not appropriate to evaluate radiogenomics studies, which mainly focus on the assessment of radiomics-genomics association. The RQS of the studies were median 15 with a range of 12 ~ 18. The RQS has 16 items grouped into 6 major categories and we assessed whether a study met the requirements of each category. We further explored the adherence rate according to the 6 key categories and 16 items (Table 3). We observed that the "high level of evidence" category was the least satisfied one and suggest future studies to move towards prospective study designs to confirm

existing retrospective design-based studies. A longitudinal study design and independent validation over many institutions are other directions that could improve the level of evidence. The "open science and data" category was the second least satisfied category. Satisfying this category is also related to the "high level of evidence" and more academic journals are mandating the policy of open data and codes.[82–84] Thus, we believe more studies will satisfy the "open science and data" category in the future.

Integration of deep learning

Radiomic studies rely heavily on machine learning and the field of machine learning is rapidly moving toward DL.[85–90] This trend also applies to medical imaging; thus, an increasing number of radiomics studies have adopted DL as the major methodological component.[91–96] Almost all conventional steps in radiomics can be replaced with DL equivalent versions. In the image acquisition step, DL can be applied to learn features that are less affected by the variability in imaging parameters.[97] In the specification of ROIs, various DL approaches, including U-net-based segmentation methods, have already been used to perform automatic tumor segmentation.[98] The performance of tumor segmentation can be measured with standard dice coefficient factoring in inter-rater variability.[99] However, the results of the DL-based automatic segmentation are still required to be confirmed by a human expert. Radiomics features are handcrafted features that are predefined based on expert knowledge. DL is capable of learning specific features from the data themselves; thus, there is no need to specify predefined features.[85] This implies that one could apply the same DL approach to solve many different tasks. However, DL can properly learn features from the data only if sufficient samples are available to train the model.[86,89,90] This could be difficult to apply in practice because the sample size requirements for deep learning are larger than those of conventional machine learning studies.

DL-derived features can lead to improved performance in many tasks, but they are difficult to interpret.[86,89,90] This "interpretability" issue is especially important in the medical domain for DL models to gain expert's trust. Recent approaches to improve "interpretability" have been actively applied in medical imaging, including gradient-weighted class activation mapping and layer-wise relevance propagation.[100] Finally, the DL method can be applied in an end-to-end manner.[85] Instead of replacing each radiomics step with a DL-based step, one big DL network can handle all steps at the same time. This can be a universal solution to the radiomics approach; however, future research is needed on the performance and the "interpretability" of this approach.

Several studies have applied DL to prostate imaging. Chaddad et al[101] created a DL model that could predict the Gleason score. Shao et al[102] developed a model that can identify tumor slices and ROIs using deep reinforcement learning. They automatically determined the most critical slice among the identified tumor slices and predicted the Gleason grades. Khosravi et al[103] conducted a study to diagnose malignancy using MRI and DL. The developed model showed results that exceeded the performance of the PI-RAD.

DL has a high potential to improve prostate radiomics. However, the issues of sample size and interpretability must be overcome. Radiomics features are mathematically defined and thus are more interpretable than data-driven DL features. A lung cancer study aiming to optimize radiotherapy dose included a neural network that tried to synthesize radiomics features in an auxiliary task.[104] Although they did not correlate DL features with radiomics features, this is one way to incorporate radiomics features into a DL network. We believe integrating or guiding the DL neural network with more interpretable radiomics features is an important future direction. In another lung cancer study, the authors tried to reduce the burden on the sample size by using a shallow network for prognosis.[105] Deep and wide networks have more capacity to learn complex representations, but for some small field of view objects, a shallow network could be suitable to extract low-level texture and edge features.[85] Thus, we believe exploring shallow networks to reduce the sample size requirements is an important direction to move forward.

Habitat and clustering

A tumor is heterogeneous in nature; one hypothesis is to assume that it consists of many subregions.[106,107] Subregions are sometimes referred to as habitats. Analyzing the subregions separately can provide more detailed information about the tumor, as compared to analyzing the whole tumor.[108–110] Habitat is commonly created by clustering; *i.e.* joining pixels with similar features. There is rich literature on how to perform clustering for various modalities and features. The concept of habitat has shown promising results in brain and breast cancer and is a promising venue for prostate radiomics.[108–110] The habitat concept can be expanded to include various prostate zones (*i.e.* anterior fibromuscular stroma and central/transitional/peripheral zones).[111] Features from the tumor habitat and the various prostate zones can be compared. The interactions among them could be a rich source of information for prostate radiomics.

Incorporating histology

The prostate is one of the few organs where whole-mount histology information is available after prostatectomy. The histology images could be reformatted into a stack of slices that can be registered on *in vivo* imaging, such as pelvic MRI. With the registration, rich features derived from the histology could be used to provide additional features for the radiomics approach. Jamshidi et al[112] showed that the combination of histological images and *in vivo* imaging enables a more in-depth understanding of tumors. This is another promising avenue for prostate radiomics.

CONCLUSION

Radiomics has made a significant impact in radiology research, including urologic radiology. It has the potential to be used as a surrogate marker in precision medicine. The studies reviewed here show that prostate radiomics is promising for many different tasks using routine imaging. However, radiomics is hampered by difficulties, as described previously. Nonetheless, recent advancements in imaging technology and machine learning will improve radiomics, making it more acceptable for clinical use. There are underexplored options in prostate radiomics such as defining

habitats or integrating imaging information from histology compared to those in other organs. Thus, these may be considered as rich avenues for future research.

FUNDING

This research was supported by the National Research Foundation (NRF2020M3E5D2A01084892), Institute for Basic Science (IBS-R015-D1), Ministry of Science and ICT (IITP-2020-2018-0-01798), IITP grant funded by the AI Graduate School Support Program (2019-0-00421), ICT Creative Consilience program (IITP-2020-0-01821), and Artificial Intelligence Innovation Hub program (2021-0-02068).

REFERENCES

1. Yip SSF, Aerts HJWL, . Applications and limitations of radiomics. *Phys Med Biol* 2016; **61**: R150–66. doi: https://doi.org/10.1088/0031-9155/61/13/R150
2. Gillies RJ, Kinahan PE, Hricak H. Radiomics: images are more than pictures, they are data. *Radiology* 2016; **278**: 563–77. doi: https://doi.org/10.1148/radiol.2015151169
3. Niaf E, Rouvière O, Mège-Lechevallier F, Bratan F, Lartizien C. Computer-aided diagnosis of prostate cancer in the peripheral zone using multiparametric MRI. *Phys Med Biol* 2012; **57**: 3833–51. doi: https://doi.org/10.1088/0031-9155/57/12/3833
4. Ganeshan B, Panayiotou E, Burnand K, Dizdarevic S, Miles K. Tumour heterogeneity in non-small cell lung carcinoma assessed by CT texture analysis: a potential marker of survival. *Eur Radiol* 2012; **22**: 796–802. doi: https://doi.org/10.1007/s00330-011-2319-8
5. Yang X, Tridandapani S, Beitler JJ, Yu DS, Yoshida EJ, Curran WJ, et al. Ultrasound GLCM texture analysis of radiation-induced parotid-gland injury in head-and-neck cancer radiotherapy: an in vivo study of late toxicity. *Med Phys* 2012; **39**: 5732–9. doi: https://doi.org/10.1118/1.4747526
6. Ganeshan B, Skogen K, Pressney I, Coutroubis D, Miles K. Tumour heterogeneity in oesophageal cancer assessed by CT texture analysis: preliminary evidence of an association with tumour metabolism, stage, and survival. *Clin Radiol* 2012; **67**: 157–64. doi: https://doi.org/10.1016/j.crad.2011.08.012
7. Acharya UR, Ng EYK, Tan J-H, Sree SV. Thermography based breast cancer detection using texture features and support vector machine. *J Med Syst* 2012; **36**: 1503–10. doi: https://doi.org/10.1007/s10916-010-9611-z
8. Cho H-H, Lee G, Lee HY, Park H. Marginal radiomics features as imaging biomarkers for pathological invasion in lung adenocarcinoma. *Eur Radiol* 2020; **30**: 2984–94. doi: https://doi.org/10.1007/s00330-019-06581-2
9. Park JE, Park SY, Kim HJ, Kim HS. Reproducibility and generalizability in radiomics modeling: possible strategies in radiologic and statistical perspectives. *Korean J Radiol* 2019; **20**: 1124–37. doi: https://doi.org/10.3348/kjr.2018.0070
10. Da-ano R, Masson I, Lucia F, Doré M, Robin P, Alfieri J, et al. Performance comparison of modified combat for harmonization of radiomic features for multicenter studies. *Sci Rep* 2020; **10**: 10. doi: https://doi.org/10.1038/s41598-020-66110-w
11. Da-Ano R, Visvikis D, Hatt M. Harmonization strategies for multicenter radiomics investigations. *Phys Med Biol* 2020; **65**: 24TR02. doi: https://doi.org/10.1088/1361-6560/aba798
12. Orlhac F, Boughdad S, Philippe C, Stalla-Bourdillon H, Nioche C, Champion L, et al. A postreconstruction harmonization method for multicenter radiomic studies in PET. *J Nucl Med* 2018; **59**: 1321–8. doi: https://doi.org/10.2967/jnumed.117.199935
13. Mahon RN, Ghita M, Hugo GD, Weiss E. Combat harmonization for radiomic features in independent phantom and lung cancer patient computed tomography datasets. *Phys Med Biol* 2020; **65**: 015010. doi: https://doi.org/10.1088/1361-6560/ab6177
14. McAuliffe MJ, Lalonde FM, McGarry D, Gandler W, Csaky K, Trus BL. Medical image processing, analysis & visualization in clinical research. *Proceedings of the IEEE Symposium on Computer-Based Medical Systems* 2001: 381–8.
15. Hill DLG, Batchelor PG, Holden M, Hawkes DJ. Medical image registration. *Physics in Medicine and Biology* 2001; **46**: 1–45.
16. Um H, Tixier F, Bermudez D, Deasy JO, Young RJ, Veeraraghavan H. Impact of image preprocessing on the scanner dependence of multi-parametric MRI radiomic features and covariate shift in multi-institutional glioblastoma datasets. *Phys Med Biol* 2019; **64**: 165011. doi: https://doi.org/10.1088/1361-6560/ab2f44
17. Traverso A, Wee L, Dekker A, Gillies R. Repeatability and reproducibility of radiomic features: a systematic review. *Int J Radiat Oncol Biol Phys* 2018; **102**: 1143–58. doi: https://doi.org/10.1016/j.ijrobp.2018.05.053
18. Fave X, Zhang L, Yang J, Mackin D, Balter P, Gomez D. Impact of image preprocessing on the volume dependence and prognostic potential of radiomics features in non-small cell lung cancer. *Translational Cancer Research* 2016; **5**: 349–63.
19. Vovk U, Pernuš F, Likar B. A review of methods for correction of intensity inhomogeneity in MRI. *IEEE Trans Med Imaging* 2007; **26**: 405–21. doi: https://doi.org/10.1109/TMI.2006.891486
20. Tustison NJ, Avants BB, Cook PA, Zheng Y, Egan A, Yushkevich PA, et al. N4ITK: improved N3 bias correction. *IEEE Trans Med Imaging* 2010; **29**: 1310–20. doi: https://doi.org/10.1109/TMI.2010.2046908
21. Shiradkar R, Ghose S, Jambor I, Taimen P, Ettala O, Purysko AS, et al. Radiomic features from pretreatment biparametric MRI predict prostate cancer biochemical recurrence: preliminary findings. *J Magn Reson Imaging* 2018; **48**: 1626–36. doi: https://doi.org/10.1002/jmri.26178
22. Krauss T, Engel H, Jilg CA, Gratzke C, Bamberg F, Benndorf M. MRI phenotype of the prostate: transition zone radiomics analysis improves explanation of prostate-specific antigen (PSA) serum level compared to volume measurement alone. *Eur J Radiol* 2020; **129**: 109063. doi: https://doi.org/10.1016/j.ejrad.2020.109063
23. Mazonakis M, Damilakis J, Varveris H, Prassopoulos P, Gourtsoyiannis N. Image segmentation in treatment planning for prostate cancer using the region growing technique. 2014; **74**: 243–8.
24. Bieniek A, Moga A. An efficient watershed algorithm based on connected components. *Pattern Recognition* 2000; **33**: 907–16.

25. Zhang Y, Matuszewski BJ, Histace A, Precioso F, Kilgallon J, Moore C. Boundary delineation in prostate imaging using active contour segmentation method with Interactively defined object regions. *Lecture Notes in Computer Science* 2010; **6367 LNCS**: 131–42.
26. Aldoj N, Biavati F, Michallek F, Stober S, Dewey M. Automatic prostate and prostate zones segmentation of magnetic resonance images using DenseNet-like U-net. *Scientific Reports* 2020; **10**: 1–17. doi: https://doi.org/10.1038/s41598-020-71080-0
27. Beig N, Khorrami M, Alilou M, Prasanna P, Braman N, Orooji M, et al. Perinodular and intranodular radiomic features on lung CT images distinguish adenocarcinomas from granulomas. *Radiology* 2019; **290**: 783–92. doi: https://doi.org/10.1148/radiol.2018180910
28. Nakayama H, Yamada K, Saito H, Oshita F, Ito H, Kameda Y, et al. Sublobar resection for patients with peripheral small adenocarcinomas of the lung: surgical outcome is associated with features on computed tomographic imaging. *Ann Thorac Surg* 2007; **84**: 1675–9. doi: https://doi.org/10.1016/j.athoracsur.2007.03.015
29. Lee AK, DeLellis RA, Silverman ML, Heatley GJ, Wolfe HJ. Prognostic significance of peritumoral lymphatic and blood vessel invasion in node-negative carcinoma of the breast. *J Clin Oncol* 1990; **8**: 1457–65. doi: https://doi.org/10.1200/JCO.1990.8.9.1457
30. Braman NM, Etesami M, Prasanna P, Dubchuk C, Gilmore H, Tiwari P, et al. Intratumoral and peritumoral radiomics for the pretreatment prediction of pathological complete response to neoadjuvant chemotherapy based on breast DCE-MRI. *Breast Cancer Res* 2017; **19**: 57. doi: https://doi.org/10.1186/s13058-017-0846-1
31. Uematsu T. Focal breast edema associated with malignancy on T2-weighted images of breast MRI: peritumoral edema, prepectoral edema, and subcutaneous edema. *Breast Cancer* 2015; **22**: 66–70. doi: https://doi.org/10.1007/s12282-014-0572-9
32. Prasanna P, Patel J, Partovi S, Madabhushi A, Tiwari P. Radiomic features from the peritumoral brain parenchyma on treatment-naïve multi-parametric MR imaging predict long versus short-term survival in glioblastoma multiforme: preliminary findings. *Eur Radiol* 2017; **27**: 4188–97. doi: https://doi.org/10.1007/s00330-016-4637-3
33. Algohary A, Shiradkar R, Pahwa S, Purysko A, Verma S, Moses D, et al. Combination of peri-tumoral and Intra-Tumoral radiomic features on Bi-Parametric MRI accurately Stratifies prostate cancer risk: a multi-site study. *Cancers* 2020; **12**: 2200. doi: https://doi.org/10.3390/cancers12082200
34. van Griethuysen JJM, Fedorov A, Parmar C, Hosny A, Aucoin N, Narayan V, et al. Computational radiomics system to decode the radiographic phenotype. *Cancer Res* 2017; **77**: e104–7. doi: https://doi.org/10.1158/0008-5472.CAN-17-0339
35. Aerts HJWL, Velazquez ER, Leijenaar RTH, Parmar C, Grossmann P, Carvalho S, et al. Decoding tumour phenotype by noninvasive imaging using a quantitative radiomics approach. *Nat Commun* 2014; **5**: 4006. doi: https://doi.org/10.1038/ncomms5006
36. Haralick RM, Shanmugam K, Dinstein I. Textural features for image classification. *IEEE Transactions on Systems, Man, and Cybernetics* 1973; **SMC-3**: 610–21.
37. Prasanna P, Tiwari P, Madabhushi A. Co-Occurrence of local anisotropic gradient orientations (collage): a new radiomics descriptor. *Scientific Reports* 2016; **6**: 1–14.
38. Ismail M, Hill V, Statsevych V, Huang R, Prasanna P, Correa R, et al. Shape features of the lesion habitat to differentiate brain tumor progression from pseudoprogression on routine multiparametric MRI: a multisite study. *AJNR Am J Neuroradiol* 2018; **39**: 2187–93. doi: https://doi.org/10.3174/ajnr.A5858
39. Grélard F, Baldacci F, Vialard A, Domenger J-P. New methods for the geometrical analysis of tubular organs. *Med Image Anal* 2017; **42**: 89–101. doi: https://doi.org/10.1016/j.media.2017.07.008
40. Alilou M, Orooji M, Beig N, Prasanna P, Rajiah P, Donatelli C, et al. Quantitative vessel tortuosity: a potential CT imaging biomarker for distinguishing lung granulomas from adenocarcinomas. *Sci Rep* 2018; **8**: 15290. doi: https://doi.org/10.1038/s41598-018-33473-0
41. Chandrashekar G, Sahin F. A survey on feature selection methods. *Computers and Electrical Engineering* 2014; **40**: 16–28.
42. Guyon I, Weston J, Barnhill S, Vapnik V. Gene selection for cancer classification using support vector machines. *Machine Learning* 2002; **46**: 389–422.
43. Significance TB. Effect sizes, stepwise methods, and other issues: strong arguments move the field. *Journal of Experimental Education* 2001; **70**: 80–93.
44. Tibshirani R. Regression selection and shrinkage via the LASSO. *Journal of the Royal Statistical Society B* 1996;.
45. Wold S, Esbensen K, Geladi P. Principal component analysis. *Chemometrics and Intelligent Laboratory Systems* 1987; **2**: 37–52.
46. Hearst MA, Dumais ST, Osuna E, Platt J, Scholkopf B. Support vector machines. *IEEE Intelligent Systems and their Applications* 1998; **13**: 18–28.
47. a L, Wiener M. Classification and regression by randomForest. *R news* 2002;.
48. FISHER RA. The use of multiple measurements in taxonomic problems. *Annals of Eugenics* 1936; **7**: 179–88.
49. Pregibon D. Logistic regression diagnostics. *The Annals of Statistics* 1981; **9**: 705–24.
50. Cox DR. Regression models and life-tables. *Journal of the Royal Statistical Society: Series B* 1972; **34**: 187–202.
51. Mazurowski MA. Radiogenomics: what it is and why it is important. *J Am Coll Radiol* 2015; **12**: 862–6. doi: https://doi.org/10.1016/j.jacr.2015.04.019
52. Kuo MD, Jamshidi N. Behind the numbers: decoding molecular phenotypes with radiogenomics--guiding principles and technical considerations. *Radiology* 2014; **270**: 320–5. doi: https://doi.org/10.1148/radiol.13132195
53. Beig N, Bera K, Prasanna P, Antunes J, Correa R, Singh S, et al. Radiogenomic-based survival risk stratification of tumor habitat on Gd-T1w MRI is associated with biological processes in glioblastoma. *Clin Cancer Res* 2020; **26**: 1866-1876. doi: https://doi.org/10.1158/1078-0432.CCR-19-2556
54. Lee HW, Cho H-H, Joung J-G, Jeon HG, Jeong BC, Jeon SS, et al. Integrative radiogenomics approach for risk assessment of post-operative metastasis in pathological T1 renal cell carcinoma: a pilot retrospective cohort study. *Cancers* 2020; **12**: E866. doi: https://doi.org/10.3390/cancers12040866
55. Choi SW, Cho H-H, Koo H, Cho KR, Nenning K-H, Langs G, et al. Multi-habitat radiomics unravels distinct phenotypic subtypes of glioblastoma with clinical and genomic significance. *Cancers* 2020; **12**: 1–15. doi: https://doi.org/10.3390/cancers12071707
56. Karlo CA, Di Paolo PL, Chaim J, Hakimi AA, Ostrovnaya I, Russo P, et al. Radiogenomics of clear cell renal cell carcinoma: associations between CT imaging features and mutations. *Radiology* 2014; **270**: 464–71. doi: https://doi.org/10.1148/radiol.13130663
57. Beig N, Patel J, Prasanna P, Hill V, Gupta A, Correa R, et al. Radiogenomic analysis of hypoxia pathway is predictive of overall survival in glioblastoma. *Sci Rep* 2018; **8**: 7. doi: https://doi.org/10.1038/s41598-017-18310-0

58. Zinn PO, Singh SK, Kotrotsou A, Hassan I, Thomas G, Luedi MM, et al. A coclinical radiogenomic validation study: conserved magnetic resonance radiomic appearance of periostin-expressing glioblastoma in patients and xenograft models. *Clin Cancer Res* 2018; **24**: 6288–99. doi: https://doi.org/10.1158/1078-0432.CCR-17-3420
59. Jamshidi N, Jonasch E, Zapala M, Korn RL, Aganovic L, Zhao H, et al. The radiogenomic risk score: construction of a prognostic quantitative, noninvasive image-based molecular assay for renal cell carcinoma. *Radiology* 2015; **277**: 114–23. doi: https://doi.org/10.1148/radiol.2015150800
60. Zhao B, Tan Y, Tsai W-Y, Qi J, Xie C, Lu L, et al. Reproducibility of radiomics for deciphering tumor phenotype with imaging. *Sci Rep* 2016; **6**: 23428. doi: https://doi.org/10.1038/srep23428
61. Constantinou C, Harrington JC, DeWerd LA. An electron density calibration phantom for CT-based treatment planning computers. *Med Phys* 1992; **19**: 325–7. doi: https://doi.org/10.1118/1.596862
62. Jackson EF, Ginsberg LE, Schomer DF, Leeds NE. A review of MRI pulse sequences and techniques in neuroimaging. *Surg Neurol* 1997; **47**: 185–99. doi: https://doi.org/10.1016/s0090-3019(96)00375-8
63. van Schie MA, van Houdt PJ, Ghobadi G, Pos FJ, Walraven I, de Boer HCJ, et al. Quantitative MRI changes during Weekly Ultra-Hypofractionated prostate cancer radiotherapy with integrated boost. *Front Oncol* 2019; **9**: 1264. doi: https://doi.org/10.3389/fonc.2019.01264
64. Clarke R, Ressom HW, Wang A, Xuan J, Liu MC, Gehan EA, et al. The properties of high-dimensional data spaces: implications for exploring gene and protein expression data. *Nat Rev Cancer* 2008; **8**: 37–49. doi: https://doi.org/10.1038/nrc2294
65. Wu W, Parmar C, Grossmann P, Quackenbush J, Lambin P, Bussink J, et al. Exploratory study to identify radiomics classifiers for lung cancer histology. *Front Oncol* 2016; **6**: 71. doi: https://doi.org/10.3389/fonc.2016.00071
66. Brown M, Bossley KM, Mills DJ, Harris CJ. High dimensional neurofuzzy systems: overcoming the curse of dimensionality. *IEEE International Conference on Fuzzy Systems* 1995: 2139–46.
67. Song J, Yin Y, Wang H, Chang Z, Liu Z, Cui L. A review of original articles published in the emerging field of radiomics. *Eur J Radiol* 2020; **127**: 108991. doi: https://doi.org/10.1016/j.ejrad.2020.108991
68. Browne MW. Cross-validation methods. *J Math Psychol* 2000; **44**: 108–32. doi: https://doi.org/10.1006/jmps.1999.1279
69. Bernatz S, Ackermann J, Mandel P, Kaltenbach B, Zhdanovich Y, Harter PN, et al. Comparison of machine learning algorithms to predict clinically significant prostate cancer of the peripheral zone with multiparametric MRI using clinical assessment categories and radiomic features. *Eur Radiol* 2020; **30**: 6757–69. doi: https://doi.org/10.1007/s00330-020-07064-5
70. Chaddad A, Kucharczyk MJ, Niazi T. Multimodal radiomic features for the predicting Gleason score of prostate cancer. *Cancers* 2018; **10**: 249. doi: https://doi.org/10.3390/cancers10080249
71. Chen T, Li M, Gu Y, Zhang Y, Yang S, Wei C, et al. Prostate cancer differentiation and aggressiveness: assessment with a radiomic-based model vs. PI-RADS V2. *J Magn Reson Imaging* 2019; **49**: 875–84. doi: https://doi.org/10.1002/jmri.26243
72. Gong L, Xu M, Fang M, Zou J, Yang S, Yu X, et al. Noninvasive prediction of high-grade prostate cancer via Biparametric MRI Radiomics. *J Magn Reson Imaging* 2020; **52**: 1102–9. doi: https://doi.org/10.1002/jmri.27132
73. Zamboglou C, Carles M, Fechter T, Kiefer S, Reichel K, Fassbender TF, et al. Radiomic features from PSMA PET for non-invasive intraprostatic tumor discrimination and characterization in patients with intermediate- and high-risk prostate cancer - a comparison study with histology reference. *Theranostics* 2019; **9**: 2595–605. doi: https://doi.org/10.7150/thno.32376
74. Hectors SJ, Cherny M, Yadav KK, Beksaç AT, Thulasidass H, Lewis S, et al. Radiomics features measured with multiparametric magnetic resonance imaging predict prostate cancer aggressiveness. *J Urol* 2019; **202**: 498–504. doi: https://doi.org/10.1097/JU.0000000000000272
75. Bourbonne V, Vallières M, Lucia F, Doucet L, Visvikis D, Tissot V, et al. MRI-derived radiomics to guide post-operative management for high-risk prostate cancer. *Front Oncol* 2019; **9**: 807. doi: https://doi.org/10.3389/fonc.2019.00807
76. Mo X, Wu X, Dong D, Guo B, Liang C, Luo X, et al. Prognostic value of the radiomics-based model in progression-free survival of hypopharyngeal cancer treated with chemoradiation. *Eur Radiol* 2020; **30**: 833–43. doi: https://doi.org/10.1007/s00330-019-06452-w
77. McCann SM, Jiang Y, Fan X, Wang J, Antic T, Prior F, et al. Quantitative multiparametric MRI features and *PTEN* expression of peripheral zone prostate cancer: a pilot study. *AJR Am J Roentgenol* 2016; **206**: 559–65. doi: https://doi.org/10.2214/AJR.15.14967
78. Stoyanova R, Pollack A, Takhar M, Lynne C, Parra N, Lam LLC, et al. Association of multiparametric MRI quantitative imaging features with prostate cancer gene expression in MRI-targeted prostate biopsies. *Oncotarget* 2016; **7**: 53362–76. doi: https://doi.org/10.18632/oncotarget.10523
79. Kesch C, Radtke JP, Wintsche A, Wiesenfarth M, Luttje M, Gasch C. Correlation between genomic index lesions and mpMRI and 68Ga-PSMA-PET/CT imaging features in primary prostate cancer. *Scientific Reports* 2018; **8**: 1–8.
80. Fischer S, Tahoun M, Klaan B, Thierfelder KM, Weber M-A, Krause BJ, et al. A Radiogenomic approach for decoding molecular mechanisms underlying tumor progression in prostate cancer. *Cancers* 2019; **11**: 1293. doi: https://doi.org/10.3390/cancers11091293
81. Park JE, Kim HS, Kim D, Park SY, Kim JY, Cho SJ, et al. A systematic review reporting quality of radiomics research in neuro-oncology: toward clinical utility and quality improvement using high-dimensional imaging features. *BMC Cancer* 2020; **20**: 1–11. doi: https://doi.org/10.1186/s12885-019-6504-5
82. Piwowar H, Chapman W. A review of journal policies for sharing research data. *Nature Precedings* 2008; **2008**: 1.
83. Pham-Kanter G, Zinner DE, Campbell EG. Codifying collegiality: recent developments in data sharing policy in the life sciences. *PLoS One* 2014; **9**: e108451. doi: https://doi.org/10.1371/journal.pone.0108451
84. Kim J, Kim S, Cho H-M, Chang JH, Kim SY. Data sharing policies of journals in life, health, and physical sciences indexed in Journal citation reports. *PeerJ* 2020; **8**: e9924. doi: https://doi.org/10.7717/peerj.9924
85. LeCun Y, Bengio Y, Hinton G. Deep learning. *Nature* 2015; **521**: 436–44. doi: https://doi.org/10.1038/nature14539
86. Ker J, Wang L, Rao J, Lim T. Deep learning applications in medical image analysis. *IEEE Access* 2017; **6**: 9375–9.
87. Razzak MI, Naz S, Zaib A. Deep learning for medical image processing: Overview, challenges and the future. In: *Lecture Notes in Computational Vision and Biomechanics*. Springer Netherlands; 2018. pp. 323–50.
88. Hosny A, Parmar C, Quackenbush J, Schwartz LH, Aerts HJWL. Artificial intelligence in radiology. *Nat Rev Cancer*

2018; **18**: 500–10. doi: https://doi.org/10.1038/s41568-018-0016-5
89. Shen D, Wu G, Suk H-I. Deep learning in medical image analysis. *Annu Rev Biomed Eng* 2017; **19**: 221–48. doi: https://doi.org/10.1146/annurev-bioeng-071516-044442
90. Mazurowski MA, Buda M, Saha A, Bashir MR. Deep learning in radiology: an overview of the concepts and a survey of the state of the art with focus on MRI. *J Magn Reson Imaging* 2019; **49**: 939–54. doi: https://doi.org/10.1002/jmri.26534
91. Lu MT, Ivanov A, Mayrhofer T, Hosny A, Aerts HJWL, Hoffmann U. Deep learning to assess long-term mortality from chest radiographs. *JAMA Netw Open* 2019; **2**: e197416. doi: https://doi.org/10.1001/jamanetworkopen.2019.7416
92. Hosny A, Parmar C, Coroller TP, Grossmann P, Zeleznik R, Kumar A, et al. Deep learning for lung cancer prognostication: a retrospective multi-cohort radiomics study. *PLoS Med* 2018; **15**: e1002711. doi: https://doi.org/10.1371/journal.pmed.1002711
93. Wang S, Shi J, Ye Z, Dong D, Yu D, Zhou M. Predicting EGFR mutation status in lung adenocarcinoma on computed tomography image using deep learning. *European Respiratory Journal* 2019; **53**.
94. Dhungel N, Carneiro G, Bradley AP. A deep learning approach for the analysis of masses in mammograms with minimal user intervention. *Med Image Anal* 2017; **37**: 114–28. doi: https://doi.org/10.1016/j.media.2017.01.009
95. Tang Z, Xu Y, Jin L, Aibaidula A, Lu J, Jiao Z, et al. Deep learning of imaging phenotype and genotype for predicting overall survival time of glioblastoma patients. *IEEE Trans Med Imaging* 2020; **39**: 2100–9. doi: https://doi.org/10.1109/TMI.2020.2964310
96. Li Z, Wang Y, Yu J, Guo Y, Cao W. Deep Learning based Radiomics (DLR) and its usage in noninvasive IDH1 prediction for low grade glioma. *Scientific Reports* 2017; **7**: 1–11.
97. Dewey BE, Zhao C, Reinhold JC, Carass A, Fitzgerald KC, Sotirchos ES, et al. DeepHarmony: a deep learning approach to contrast harmonization across scanner changes. *Magn Reson Imaging* 2019; **64**: 160–70. doi: https://doi.org/10.1016/j.mri.2019.05.041
98. Schelb P, Kohl S, Radtke JP, Wiesenfarth M, Kickingereder P, Bickelhaupt S, et al. Classification of cancer at prostate MRI: deep learning versus clinical PI-RADS assessment. *Radiology* 2019; **293**: 607–17. doi: https://doi.org/10.1148/radiol.2019190938
99. Meyer A, Chlebus G, Rak M, Schindele D, Schostak M, van Ginneken B, et al. Anisotropic 3D multi-stream CNN for accurate prostate segmentation from multi-planar MRI. *Comput Methods Programs Biomed* 2021; **200**: 105821. doi: https://doi.org/10.1016/j.cmpb.2020.105821
100. Selvaraju RR, Cogswell M, Das A, Vedantam R, Parikh D, Batra D. Grad-CAM: visual explanations from deep networks via Gradient-Based localization. *International Journal of Computer Vision* 2020; **128**.
101. Chaddad A, Kucharczyk MJ, Desrosiers C, Okuwobi IP, Katib Y, Zhang M, et al. Deep radiomic analysis to predict gleason score in prostate cancer. *IEEE Access* 2020; **8**: 167767–78. doi: https://doi.org/10.1109/ACCESS.2020.3023902
102. Shao L, Yan Y, Liu Z, Ye X, Xia H, Zhu X, et al. Radiologist-like artificial intelligence for grade group prediction of radical prostatectomy for reducing upgrading and downgrading from biopsy. *Theranostics* 2020; **10**: 10200–12. doi: https://doi.org/10.7150/thno.48706
103. Khosravi P, Lysandrou M, Eljalby M, Li Q, Kazemi E, Zisimopoulos P. A deep learning approach to diagnostic classification of prostate cancer using pathology–radiology fusion. *Journal of Magnetic Resonance Imaging* 2021: jmri.27599.
104. Lou B, Doken S, Zhuang T, Wingerter D, Gidwani M, Mistry N, et al. An image-based deep learning framework for individualising radiotherapy dose: a retrospective analysis of outcome prediction. *The Lancet Digital Health* 2019; **1**: e136–47. doi: https://doi.org/10.1016/S2589-7500(19)30058-5
105. Mukherjee P, Zhou M, Lee E, Schicht A, Balagurunathan Y, Napel S, et al. A shallow convolutional neural network predicts prognosis of lung cancer patients in multi-institutional CT-Image data. *Nat Mach Intell* 2020; **2**: 274–82. doi: https://doi.org/10.1038/s42256-020-0173-6
106. Fidler IJ. Tumor heterogeneity and the biology of cancer invasion and metastasis. *Cancer Res* 1978; **38**: 2651-60.
107. Gerlinger M, Rowan AJ, Horswell S, Math M, Larkin J, Endesfelder D, Gronroos E, et al. Intratumor heterogeneity and branched evolution revealed by multiregion sequencing. *N Engl J Med* 2012; **366**: 883–92. doi: https://doi.org/10.1056/NEJMoa1113205
108. Cui Y, Tha KK, Terasaka S, Yamaguchi S, Wang J, Kudo K, et al. Prognostic imaging biomarkers in glioblastoma: development and independent validation on the basis of multiregion and quantitative analysis of Mr images. *Radiology* 2016; **278**: 546–53. doi: https://doi.org/10.1148/radiol.2015150358
109. Wu J, Cao G, Sun X, Lee J, Rubin DL, Napel S, et al. Intratumoral spatial heterogeneity at perfusion MR imaging predicts recurrence-free survival in locally advanced breast cancer treated with neoadjuvant chemotherapy. *Radiology* 2018; **288**: 26–35. doi: https://doi.org/10.1148/radiol.2018172462
110. Park JE, Kim HS, Kim N, Park SY, Kim Y-H, Kim JH. Spatiotemporal heterogeneity in multiparametric physiologic MRI is associated with patient outcomes in IDH-wildtype glioblastoma. *Clin Cancer Res* 2021; **27**: 237–45. doi: https://doi.org/10.1158/1078-0432.CCR-20-2156
111. De Marzo AM, Platz EA, Sutcliffe S, Xu J, Grönberg H, Drake CG, et al. Inflammation in prostate carcinogenesis. *Nat Rev Cancer* 2007; **7**: 256–69. doi: https://doi.org/10.1038/nrc2090
112. Jamshidi N, Margolis DJ, Raman S, Huang J, Reiter RE, Kuo MD. Multiregional radiogenomic assessment of prostate microenvironments with multiparametric MR imaging and DNA whole-exome sequencing of prostate glands with adenocarcinoma. *Radiology* 2017; **284**: 109–19. doi: https://doi.org/10.1148/radiol.2017162827